Harmonization of Interlaboratory X-ray Fluorescence Measurement Uncertainties

Detailed Discussion Paper

Prepared by:

W. F. Gutknecht
J. B. Flanagan
A. McWilliams

RTI International
3040 Cornwallis Road
Research Triangle Park, NC 27709

Prepared for:

Office of Research and Development
U.S. Environmental Protection Agency
Research Triangle Park, NC 27709
Attn: Ms. Joann Rice, Project Officer

August 4, 2006

Table of Contents

List of Tables

List of Figures

Harmonization of Interlaboratory X-ray Fluorescence Measurement Uncertainties

Introduction

There are several contributors to total x-ray fluorescence (XRF) uncertainty as illustrated in Table 1. First, uncertainty arises from the process of determining the magnitude of a peak signal that represents a particular element. This process is usually accomplished by some form of iterative peak or curve fitting process. The uncertainty varies from greater than 100% near the detection limit to less then 5% at high levels; at higher concentration, it is generally a function of the square root of n, the number of x-rays counted under the peak. The magnitude of this effect goes down with increasing concentration. Uncertainty is increased if deconvolution of overlapping peaks is required. There is general agreement upon values for two other sources of uncertainty, which are calibration and field sampling; the uncertainty values for these two parameters have been estimated as a maximum of 5% of measured concentration. Some of the factors listed in Table 1, such as Sampler Flow Rate and Sample Deposit Area are subsumed into the calibration and field sampling terms.

The next contributor to uncertainty to be considered, and the main topic of this white paper, is attenuation. Attenuation occurs when incoming (excitation) x-rays are absorbed by the sample before causing fluorescence and when outgoing (fluorescent) x-rays are absorbed by the sample before escaping the sample. One net effect is that the instrument "senses" less signal from an element than would be expected. This effect is most significant for the lighter elements, Na, Mg, Al, Si, P, S, Cl, K, and Ca, which are excited by and emit lower energy or "soft" x-rays. Experts in this field who were considered for this white paper, Robert Kellogg, Rick Sarver, Bob Eldred, Paul Wakabayashi, John Cooper, Warren White, and Tom Dzubay (deceased), all identify attenuation as the principle source of uncertainty for the light elements, except for the uncertainty of peak area determination at low concentrations.

1.0 DETERMINATION OF FIELD SAMPLE ATTENUATION/X-RAY FLUORESCENCE UNCERTAINTY

1.1 Work of Dzubay and Nelson

Dzubay and Nelson[1] calculated attenuation values separately for "fine" and "coarse" particles based on reports in the literature in the 70's of a bimodal distribution of particle volume

Table 1. Sources of uncertainty included by different laboratories

Uncertainty Source Category	Uncertainty Source Sub-Category	RTI International	Chester LabNet	Cooper Environmental Services	Robert Kellogg EPA (Alion Science)	UC Davis IMPROVE
Peak Fit (area/height) Coefficient Uncertainty	**Regression based**	- - -	- - -	1% to 100% for regression based (peak size dependent)	~ 1 to ∞% (peak size dependent)	Calculated from fit
	Photon count based (Poisson)	Calculated from Poisson statistics	Poisson	1% to 100% (peak size dependent)	- - -	Poisson
Calibration Uncertainty	**Based on reported or measured NIST SRM uncertainty**	Currently not applied	5% for all elements	- - -	Not applied	Not applied
	Based on multipoint calibration curve regression	- - -	- - -	Applied to estimated uncertainty, ≤2%	2.3 to 4.5% (element specific) **[Note 1]**	4% for all elements
Attenuation with Calibration Standard [Note 2]	**(Z=11-14)**	Currently not applied	Self-absorption and particle size based on SRM2783	Self-absorption correction but no self-absorption uncertainty	Mass-based using XRF analysis results, ~0 – 3%	Not applied – thin foil standards used
	(Z>14)	Currently not applied	Self-absorption up to Z=20	Self-absorption correction for up to Z = 26 (Fe) but no self-absorption uncertainty	Mass-based using XRF analysis results, <<1%	Not applied – thin foil standards used

Attenuation with Field Sample [Note 2]	**(Z=11-14)**	Currently not applied	Self-absorption and particle size	Self-absorption correction but no self-absorption uncertainty	Particle-based, 6% to 3%	Particle based, 22% to 8%
	(Z>14)	Currently not applied	Self-absorption up to Z=20 (Ca)	Self-absorption correction for up to Z = 26 (Fe) but no self-absorption uncertainty	Mass-based using XRF analysis results, <1%	Particle based, <2%
Interference, e.g., Rb on Si [Note 3]	- - -	Currently not applied	See equation 4 Section 9.4 SOP XR-005.01	Included in peak fit coefficient uncertainty	Depends on interfering element conc. and uncertainty	Not applied
Monitor Detector [Note 4]	- - -	Currently not applied	Not applied	<1%	<1%	Not applied
Sampler Flow Rate	- - -	Included in 5% total field variability **[Note 5]**	Not applied	Not applied	2 to 5%	3%
Sample Deposit Area	- - -	Included in 5% total field variability **[Note 5]**	Not applied	Not applied	Average 2%	Included in 3% flow variability

Notes:

[1] - Kellogg uses inter-element regression to further minimize calibration uncertainty below levels achievable with a single-element standard.

[2] - The type of attenuation correction assumed -- particle size or mass -- should be specified.

[3] - This consists of interferences that are not included in the "Fit Coefficient" uncertainty calculation.

[4] - Variability in monitor sensitivity that is not captured in direct determination of calibration uncertainty, for example long term drift and instability between calibrations.

[5] - RTI includes 5% of the final concentration value to all uncertainties (for XRF, as well as for IC, OC/EC, and gravimetry) to account for all components of "field" variability. These include flow/volume, deposit area, and handling effects.

(Figure 1) as a function of diameter. Dzubay and Nelson (and also Robert Kellogg) have defined "coarse" as the particles in size between $PM_{2.5}$ and PM_{10}, i.e., $PM_{2.5-10}$; here, $PM_{2.5}$ particles are those less than 2.5 µm in aerodynamic diameter and PM_{10} are those less than 10 µm in aerodynamic diameter. Dzubay and Nelson noted that fine particles were attributed to aerosol growth by gas-to-particle conversion and coagulation such that the particles would be expected to be similar in composition. On the other hand, coarse particles were attributed to breakdown of larger particles by mechanical processes (grinding, abrasion), such that their composition would be diverse.

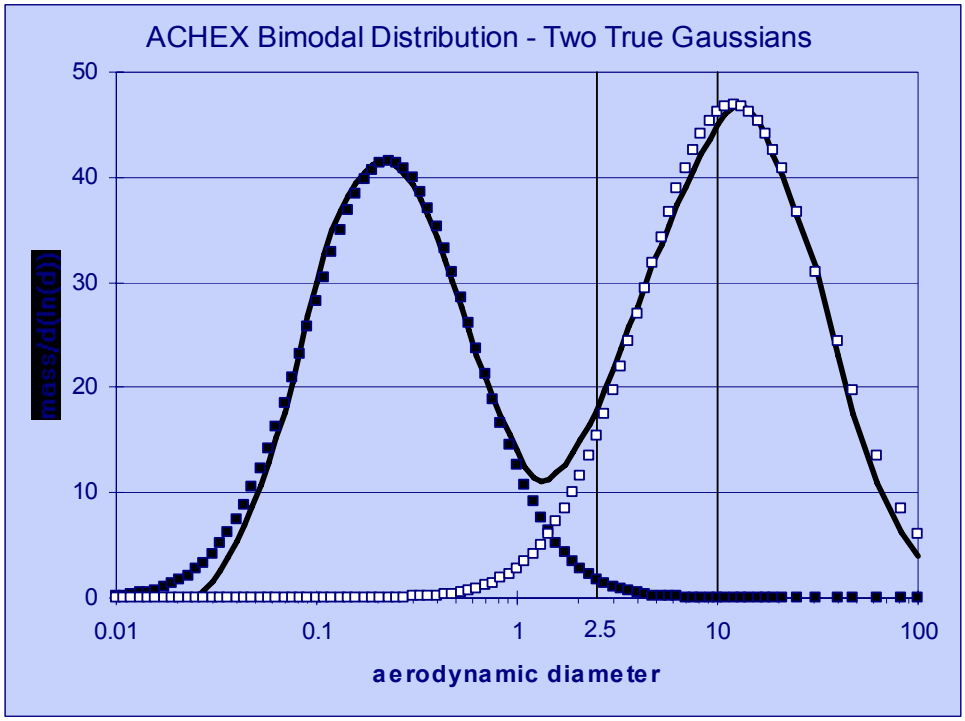

Figure 1. Particle Size Distributions for Fine and Coarse Particles. (white squares = $PM_{2.5-10}$ + >10 µm; black squares = $PM_{2.5}$; black line = total, as measured)

1.1.1 Fine Particles

If the x-ray absorption is negligible within individual particles and the particle diameter is small compared to the thickness of the layer, then the sample can be considered homogeneous.[2] Dzubay and Nelson assumed this was the case for fine particles, and therefore the attenuation, A, for a homogeneous layer with mass per unit area, *m*, on the surface of the filter is

$$A = [1-\exp(-\underline{\mu}\, m)]/\underline{\mu}\, m \qquad (1)$$

where m = areal density of the deposit (gm/cm^2)

A = mass absorption

e = natural log exponent (mathematical e)

$\underline{\mu}$ = total mass absorption coefficient (cm^2/gm)

Now $\underline{\mu} = (\mu \csc\theta + \mu' \csc\theta')$ (2)

where θ = the angle at which upcoming x-rays strike the sample

θ' = angle at which the exiting x-rays travel to the detector

Now $$\mu = \sum\left(\mu_i w_i\right) \quad (3)$$

where μ = the total mass absorption coefficient of all elements present on the incoming X-rays (cm^2/g)

μ_i = the mass absorption coefficient of each element i on the incoming X-rays

w_i = the weight fraction of element i in the deposit ($0 < w_i < 1$)

and,

$$\mu' = \sum\left(\mu_{ij} w_i\right) \quad (4)$$

where μ' = the total mass absorption coefficient of all elements present on the exiting (fluorescing) X-rays for element j

μ_{ij} = the mass absorption coefficient of each element i on the exiting X-rays from element j.

The values for μ_i and μ_{ij} are dependent upon the energy of the excitation x-rays and the x-ray energies of the element emissions as shown in the table in Attachment 1. An up-to-date listing of attenuation coefficients can be found on line. These tables are published by J. H. Hubbell and S. M. Seltzer of NIST and can be found on-line at http://physics.nist.gov/PhysRefData/XrayMassCoef/cover.html.

The calculation becomes more complex if one assumes that the particles penetrate into the porous filter to some extent. This contribution to attenuation was only considered by Dzubay and Nelson. However, the concept of attenuation by the filter itself is presented to further describe the complexity of the attenuation process. The concentration as a function of depth, *h*, would be expected to have an exponential decay of the form

$$c(h) = \exp\left[h\ \ell n(P)/t\right]$$

where

P = fractional penetration through the entire filter (0 < P <1)

t = thickness of the filter

Then A(filter) = $\left[1 - P\exp\left(\mu_F m_F\right)\right]/\left[\left(1-P\right)\left(1 - \mu_F m_F / \ln P\right)\right]$ (5)

where

A(filter) = attenuation factor for the filter

μ_F = mass absorption coefficient for the filter medium (cm^2/g)

m_F = mass per unit area of the filter (g/cm^2)

Then A(total) = A(layer) A(filter) (6)

where

A(total) = attenuation factor for the filter plus the collected deposit

Dzubay and Nelson calculated values for A for a cellulose membrane filter following Equation 5 and for layers of light elements following Equation 1; results are presented in Table 2. For this calculation, the area density of the cellulose membrane filter was taken as 0.005 g/cm^2 and P was taken as 0.1%. We see that the attenuation can be quite high for the filter. However, it should be noted that the penetration with Teflon filters should be less; Lockhart[3] et al. reported P values of 0.01% to 0.02% for Millipore membranes, which would result in less attenuation. The uncertainties shown for the filter attenuation values are derived from ranging the P value from 0.002% to 1%. Dzubay and Nelson stated that more research was needed before corrections for particle penetration could be made with confidence. According to Robert Kellogg, penetration for each element can actually be calculated by measuring the x-ray intensity from the front and back sides of the filter; he has done this in the past with quartz filters but is unaware of it being done with Teflon filters.

The attenuations for the light elements were calculated using the concentrations given in Table 3. The remaining 81.4% of the filter loading mass (Z < 13), after accounting for the seven elements measured and the other elements with Z > 13, was assigned to $C_6H_{10}O_5$. It should be noted that a heavily loaded STN filter would be around 0.1 mg/cm^2 total fine particulate mass, not counting the mass of the Teflon filter; a more typical filter loading would be less than this and so the estimated attenuation for the STN would be in the range of the values for "Layer 0.1 mg/cm^2" shown in Table 2, e.g., about 0.90 for Mg. One can see the significant effect on attenuation of the loading going from 0.1 mg/cm^2 to 0.5 mg/cm^2. The uncertainty values presented for the "Layer 0.5 mg/cm^2" were determined from the range of the attenuations

resulting from the 81.4%, unmeasured light material varying from $C_6H_{10}O_5$ to only O. The changes in attenuation associated with this large change in composition for the organic/carbonaceous phase are small for all but the lightest elements.

Table 2. Calculated attenuation factors (A) for x-ray excitation of K_α radiation of light elements in a filter and in fine particles considered a homogeneous layer

Element	Cellulose[a] filter	Layer[b] 0.1 mg/cm^2	Layer[b] 0.5 mg/cm^2
Mg	0.40 ± 0.11	0.90	0.61 ± 0.10[c] (16%)
Al	0.52 ± 0.11	0.93	0.72 ± 0.08 (11%)
Si	0.62 ± 0.10	0.95	0.79 ± 0.06 (7.6%)
P	0.71 ± 0.08	0.96	0.83 ± 0.04 (4.8%)
S	0.78 ± 0.06	0.97	0.87 ± 0.03 (3.4%)
Cl	0.83 ± 0.06	0.96	0.83 ± 0.02 (2.4%)
K	0.89 ± 0.04	0.98	0.89 ± 0.01 (1.1%)
Ca	0.91 ± 0.04	0.98	0.90 ±0.01 (1.1%)
K*	0.92 ± 0.03	0.98	0.92 ± 0.01 (1.1%)
Ca*	0.94 ± 0.03	0.99	0.94 ± 0.01 (1.1%)
Ti*	0.97 ± 0.02	0.99	0.96 ± 0.00 (0%)

[a]Areal density is 5 mg/cm^2; P = 0.1% and ranging from 0.002% to 1%.
[b]The composition is 81.4% cellulose plus the fine particle elemental concentrations listed in Table 3; no uncertainty was published for this layer.
[c]The stated uncertainty represents a major change in the composition as directed in the text.
*Excitation with 18 KeV x-rays; other elements in list are excited with 4.5 KeV x-rays.
Note: STN uses Teflon, not cellulose. A heavily loaded STN filter would be around 0.1 mg/cm^2 total fine particulate mass, not counting the mass of the Teflon filter; a more typical filter would be less than this.

Table 3. Percentage composition by weight of aerosol collected by a dichotomous sampler in a St. Louis residential neighborhood in August 1973 and analyzed by x-ray fluorescence.

Element	Fine, %
Si	1.5
S	12.7
Ca	0.4
Ti	0.2
Fe	0.5
Br	0.4
Pb	1.8
other Z>13	1.1
other Z<13	81.4

1.1.2 Coarse Particles

Dzubay and Nelson also determined attenuation for the coarse particles. They assumed the particles were collected as a monolayer and that the particles were equivalent spheres. Then,

$$A(\text{sphere}) = (3/2Y^3)[Y^2 - 2 + (2Y + 2)\exp(-Y)]\,[\exp(-KY\,(\Theta + \Theta')^2)] \qquad (7)$$

where,

$K = 4\text{x}10^{-6}\ (\text{degrees})^{-2}$

$Y = (\mu + \mu')\,d\rho$

μ and μ' are the mass absorption coefficients for the incident and fluorescent radiation

d = geometrical particle diameter (cm)

ρ = density of the particle (g/cm^3)

θ = the angle at which upcoming x-rays strike the sample (degrees)

θ' = angle at which the exiting x-rays travel to the detector (degrees)

To compute the net attenuation for the sample, A(sphere) must be averaged over the size distribution on the filter.

$$A(\text{Coarse}) = [\int_0^\infty A(\text{sphere})\,dV/dD\,T(D)\,dD]/\,[\int_0^\infty dV/dD\,T(D)\,dD] \qquad (8)$$

where,

dV/dD = the particle volume distribution as a function of the aerodynamic diameter D

$D = d\,S^{½}$, where S is the specific gravity of the particle

T(D) = relative particle collection efficiency (see "y" axis, Figure 1)

It is assumed that the particles have a log-normal distribution of the form,

$$dV/dD = (1/D)\exp-[\ln(D/D_p)\,((\ln 2)^{1/2}/\ln(W)^{1/2}]^2 \qquad (9)$$

where,

D = aerodynamic diameter, cm

D_p = aerodynamic diameter corresponding to the peak of the distribution

W = full width of the distribution peak at half maximum

Values of attenuation for the coarse particles were calculated. The assumptions were that W = 5 and D_p = 10 μm and that the particles were made up of crustal materials ranging from botanical (95.7% $C_6H_{10}O_5$, 2% Ca, 1.5% K, 0.6% Mg, 0.2% P, and 0.03% Fe) to gypsum ($CaSO_4 \cdot 2H_2O$) to almandine ($Fe_3Al_2Si_3O_{12}$). The actual values were calculated corresponding to composition being midway between the botanical and almandine; the exceptions are Al and Si where quartz and not botanical was considered the upper limit. Values are shown in Table 4. The uncertainties were calculated from these ranges and are numerically equal to the half width of the attenuations at the extremes of composition. Note how much larger A is for the lower energy ("softer") x-ray excitation beam.

Table 4. Attenuation for K_α x-rays of various elements in coarse particles ($PM_{2.5-10}$) for composition halfway between botanical and almandine (quartz and almandine for Al and Si).

Element	Attenuation (4.5KeV excitation)	Element	Attenuation (18 KeV excitation)
Al	0.41±0.12	K	0.83±0.13
Si	0.48±0.15	Ca	0.86±0.10
P	0.58±0.24	Ti	0.87±0.10
S	0.64±0.22	V	0.90±0.08
Cl	0.70±0.20	Cr	0.92±0.07
K	0.78±0.15	Mn	0.93±0.06
Ca	0.81±0.13	Fe	0.94±0.05
---	---	Ni	0.96±0.03
---	---	Cu	0.94±0.06
---	---	Zn	0.95±0.05

1.1.3 Summary

Dzubay and Nelson proposed that the two methods described above be used for the fine and coarse particles, respectively. It should be noted that when the calculation procedures for the coarse particles were applied to the fine particles, the attenuation was only about 2% for the lightest elements, indicating that the homogeneous layer model is best for these fine particles. They also noted that reasonable changes in the composition of the coarse particles would change these estimates for the attenuation and attenuation uncertainty. They suggested that

the calculation be iterative with recalculation after the initial elemental composition is determined. It should be noted that Robert Kellogg has changed and expanded the software used by Dzubay. Kellogg has always interpreted the coarse attenuation factor as a hard constant number. He states that it would be difficult to implement an iterative procedure for coarse particles with the current software. His choice would be to perform periodic examination of samples on a regional basis and so choose the mineral set identified as the basis for the attenuations.

1.2 Work of Bob Eldred, University of California – Davis

Like Dzubay and Nelson, Bob Eldred[4] (UC-Davis, retired) considered both particle size and mass/composition in his calculations of attenuation.

1.2.1 Attenuation Due To Particle Size

His first assumption is that the attenuation of an x-ray passing into a block of a single element of density, ρ, for a distance, *t*, is

$$A = \exp(-\mu\rho t)$$

where again, μ = the mass attenuation coefficient (cm^2/g)

Particle size. Starting with this model, he calculated the attenuation within a particle for the incident and emitted x-ray. He assumed the relation is approximately independent of the shape of the particle and is valid for a sphere though his model assumes the particle is a cube. He also assumed that the orientation of the excitation x-ray tube and detector are not significant as long as both face the "front" surface of the particle; he assumes both are in the same location. With these assumptions,

$$A= (1-\exp[-(\mu-\mu')\rho t]/(\mu-\mu')\rho t \qquad (11)$$

where, as above, μ and μ' are the mass attenuation coefficients for the incident and emitted x-rays. To determine actual attenuation for a real sample, it is necessary to integrate this equation over the distribution of the sizes of the particles. If *t* is the physical diameter, then the aerodynamic diameter is related by the density as

$$a = t\rho^{1/2}$$

Defining *F(a)* as the mass distribution of the particles containing the element of interest as a function of the particle size, *a*, the attenuation due to particles in the overlapping regions of the fine and course particles is determined as

$$A = \{\int F(a)((1-exp[-(\mu+\mu')\rho^{1/2}a])/((\mu+\mu')\rho^{1/2}a))\, da\}/\int F(a)\, da \qquad (12)$$

where the integration limits are apparently from about 0.02 μm to 12 μm and density, ρ, is based upon the assumed composition of the element-containing particle as described below.
For *F(a),* it is assumed that the particles follow a bimodal distribution (fine particles and coarse particles), where the distributions are log-normal Gaussians centered on 0.23 μm and 12 μm. Different than Dzubay and Nelson, Eldred assumes that the fine particle fraction is actually a mix of coarse and fine since there is overlap as seen in Figure 1. Also, it should be noted that "coarse" as defined by Eldred includes the aerodynamic range of 2.5 μm to approximately 100 μm; this definition, however, is not critical to his approach in that he is only concerned with the overlap of the coarse particles with the $PM_{2.5}$ distribution. Based on real-world data, the weights of the elements are assumed to be distributed between the two types:

- 0% fine + 100% coarse for soils elements Mg, Al, Si, Ca, Ti;
- 33% fine + 67% coarse for P, Na, and Cl;
- 10% fine + 90% coarse for K
- 5% fine + 95% coarse for Fe;
- 20% fine + 80% coarse for Ni, V, Cu (tentative); and
- 83% fine and 17% coarse for all others, including S.

The mean aerodynamic diameter is calculated for fine and coarse for each of the two distributions. For example, the mean aerodynamic diameter for a fine particle with an 83% fine distribution is estimated to be 0.37 μm.

Particle Composition. Particle composition affects the particle density, ρ, and so particle composition must be considered to calculate attenuation, A, presented above. Eldred, in his most recent work, assumed the composition ranges from a single element as an oxide to a mixture of all soil elements. From the IMPROVE 2000 data, he estimated an average soil particle would be:

50% O + 24% Si + 11% Al + 3% K + 5% Ca + 6% Fe + 0.6% Ti + 0.1% Mn

Net Result. The attenuation values were calculated using Equation 12 for the different elements assuming both simple oxide and soil composition and the log-normal distribution of particle size described above. Values are presented in Table 5.

Table 5. Particle size matrix attenuations for particles using XRF with Cu anode x-ray source.

Element	Fine Particle Percent	Matrix	Attenuation
Al	0%	Al_2O_3	0.85 (15%)
	0%	Al soil	0.84 (16%)
Si	0%	SiO_2	0.91 (9%)
	0%	Si soil	0.85 (15%)
K	10%	K_2O	0.98 (2%)
	10%	K soil	0.97 (3%)
Ca	0%	CaO	0.96 (4%)
	0%	Ca soil	0.95 (5%)
Fe	5%	Fe_2O_3	0.96 (4%)
	5%	Fe soil	0.99 (1%)
S	83%	$(NH_4)_2SO_4$	0.99 (1%)
	83%	H_2SO_4	0.99 (1%)

1.2.2 Attenuation Due to Sample Mass

This section describes the model for the attenuation arising from the elements being within a uniform layer of material. Eldred assumes that for this correction, the uniform layer is composed of closely-pack, well-integrated particles, and accordingly, most of the particles would be considered arising from the fine particle fraction. Here the attenuation is calculated according to Equation 1 given above. Eldred calculated the area mass density by summing all the uncorrected concentrations from the primary lines of the elements measured and multiplying the sum by a preset constant. Based on previous field studies, he assumed this factor was “7.” That is, the gravimetric mass was generally about 7 times the sum of the masses of the elements measured by XRF.

The second requirement was to estimate the composition of the material in order to calculate the total mass attenuation (absorption) coefficients per Equations 3 and 4 given above. In his most recent work, he calculated an average composition using all data collected in 2002 from the IMPROVE network. Here he estimated these from the nitrate (IC), carbon (OC/EC) and the assumed ammonium and oxide components of measured variables. His estimates for average composition are presented in Table 6.

Table 6. Average composition of $PM_{2.5}$ particles for 15,000 samples collected in 2002 in IMPROVE.

Element	µg/filter	Composition
H	9.3	4.8%
C	48	25.3%
N	29	15.1%
O	73	38.0%
S	18	9.4%
Al	2.8	1.45%
Si	6.2	3.19%
K	1.5	0.78%
Ca	1.7	0.86%
Fe	1.6	0.85%
Ti	0.15	0.08%
Zn	0.11	0.06%
V to Sr	0.02	<0.05%

Note: The concentration of N was estimated from nitrate, carbon, and the assumed ammonium component of sulfate and nitrate. The concentration of O was estimated from nitrate, carbon, and elements. All other variables were directly measured. The data set includes all samples in which H, C, nitrate, and the major elements were all found.

It is very interesting to note that Eldred's total for H, C, N, and O, which in Table 6 is 83.2%, agrees very well with the value given for Z < 13 by Dzubay and Nelson in Table 3 above of 81.4%. Mass (uniform layer) attenuation coefficients were calculated assuming this composition, and values for attenuation from sample mass were calculated as shown in Table 7.

Table 7. Attenuations for the Cu-anode XRF system for the median and 90th percentile $PM_{2.5}$ masses in the IMPROVE network. Corrections for all other elements are less than 1% at the 90th percentile mass (Eldred).

	Mass	Table	Na	Al	Si	S	Cl	K	Ca
50%	0.14 µg/filter	Cu-anode	0.93	0.97	0.98	0.99	0.99	0.99	0.99
90%	0.42 µg/filter	Cu-anode	0.91	0.92	0.94	0.97	0.97	0.98	0.98

1.2.3 Total Attenuation

In his earlier work, Eldred applied both the particle effect and mass effect to determine attenuation. Combining effects was apparently done by multiplying the attenuation values arising from the particle and uniform layer models. In the cited note, however, he shows data that indicate that for the coarse samples, very few samples would have enough material to cover the particles. That is, the particles can be considered free standing and not buried in a homogeneous layer. He has left this issue unresolved. Finally, Eldred does not calculate uncertainties for the attenuation values.

1.3 Work by Robert Kellogg, Alion Science and Technology

Robert Kellogg[5,6] has extended the work of Dzubay and Nelson to calculate the attenuations for the light elements taking into consideration particle size, mass, and composition. He assumes that Na through Si (Z = 11 to 14) are concentrated in the coarse particle tail and are present on the filter in a size range of ~1 to 2.5 μm. He ignores the combustion-source fine particles for these elements, if there are any. If an air shed contains a fume (or exceedingly small particles) of these elements, then his attenuation factors will cause concentrations to be too high, though this is not considered a significant risk. If he has prior knowledge that such a fume is indeed the dominant source, then his software easily allows a change in the model for Na through Si to the homogeneous model.

1.3.1 Attenuation Due To Particle Size

Kellogg calculates the attenuations for Na, Mg, Al, and Si as only due to particle size. The calculations are performed using the mathematics employed by Dzubay and Nelson, i.e., Equations 7, 8 and 9 above. What is new in this work is that Kellogg has investigated and determined most all the possible mineral forms that could include these elements, for example, aluminum silicate, magnesium silicate, quartz, and so forth. In total, 46 different minerals in 2 to 3 different size distributions have been identified. Kellogg uses the models for particles and applies them to particles of these minerals; the attenuation for each of the four elements is calculated for each particle type that includes that element over the range of particle volumes described by the log-normal size distribution found in real-world sampling. The average of the maximum and minimum attenuation values for each element is taken as the attenuation for that element in the sample; the uncertainty is based on the range of attenuation over the mineral set. Kellogg considers the mineral set comprehensive and the uncertainty is therefore expected to accurately represent the range of attenuations, and therefore is assumed to be 2.5 σ. Values

for attenuation provided by Kellogg (Personal communication and Reference 6) using two different x-ray instruments are shown in Table 8.

Table 8. Attenuation values ± 1σ for coarse particles based on averaging attenuations for different potential mineral forms containing the element

Atomic number, Z	Element	Al fluorescer, Kevex XRF (coarse fraction that overlaps fine fraction)	Ti fluorescer, Kevex XRF (coarse fraction that overlaps fine fraction)	LBL XRF ($PM_{2.5-10}$)
11	Na	0.620 ± 0.036 (5.8%)	---	---
12	Mg	0.650 ± 0.044 (5.2%)	---	---
13	Al	---	0.760 ± 0.032 (4.3%)	0.753 ± 0.032 (4.2%)
14	Si	---	0.780 ± 0.020 (2.6%)	0.796 ± 0.032 (4.0%)
15	P	---	---	---
16	S	---	---	---
17	Cl	---	---	---
19	K	---	---	---
20	Ca	---	---	---

1.3.2 Attenuation Due to Sample Mass

Kellogg uses the homogeneous layer-based attenuation model (Equation 1 above) for Z>14. The attenuation is composition- and areal-density dependant so it is calculated on each sample. The non-analyzable portion is reported by Kellogg as 50% to 90% of the sample; this is principally C, H, N, and O. The mass of this unknown composition is calculated as (Gravimetric Total – Mass of the Measured Elements). Kellogg goes through an iterative process to determine the attenuation:

- The concentration of each element in the sample is calculated without attenuation correction
- The “unknown material” mass for the sample is calculated as (Total Gravimetric Mass – Sum of All Measured Element Masses)
- Attenuation is calculated for each element based on the mass on the filter, the type of x-ray fluorescer, and the “raw” concentrations of each element measured assuming the unknown mass is $C_6H_{10}O_5$.

- The concentration of each element that has been adjusted upward due to the attenuation correction is then used to repeat the calculation to determine new attenuation values

- This cycle is repeated until attenuations for all elements change by less than 0.01%

- The process is now repeated using C_6H_6 as the unknown mass and a second set of attenuation values are determined

- Finally, the unknown mass is taken as O (oxygen) and a third set of attenuation values is determined.

The average of the attenuation values measured under these three assumptions is taken as the "true" attenuation for the sample. The span of attenuations provides the measure of uncertainty. Kellogg assumes the uncertainty calculated is 3 σ because of the "extreme" assumptions about the composition of the unknown mass of the sample. One of the outcomes of this approach is that the attenuation varies with the sample. Table 9 presents average attenuation and uncertainty values for 18 real-world samples. One can see that there is a fairly wide variation in the attenuation uncertainty from sample to sample for the elements P through Ca, but the absolute values are quite low, less than 1%.

1.4 John Cooper of Cooper Environmental Services

John Cooper[7] does not apply particle size correction factors, in part because they are expected to be small for $PM_{2.5}$ filter deposits based on Dzubay's work. Cooper does apply absorption corrections to all elements with atomic number up to Fe. These corrections are based on reported PM mass, Dzubay's correction factors, and the assumption of a uniform deposit, which is not always the case. His values are approximations since Dzubay's absorption coefficients are based on an assumed composition and excitation conditions. For example, Cooper does not use secondary (fluorescer) excitation as did Dzubay. Cooper does not calculate uncertainties for the elements corrected because he believes the models assuming that non-measurable components vary from C_6H_{10} to oxygen or that the mineral composition covers the full potential range are not justified, and research focused on these parameters is necessary before their application is justified. He does acknowledge, however, that uncertainties for elements like Al and Si can dominate the uncertainty for these low atomic number elements. Consequently, when uncertainties for the light elements from the Cooper laboratory are compared with those from Chester, described in the next section, Cooper's are significantly lower.

Table 9. Average attenuation and attenuation uncertainty for eighteen (18) samples assuming the homogeneous layer model with non-XRF material ranging from $C_6H_{10}O_5$ to C_6H_6 to O (all oxygen)

Element	Average Attenuation	Average Uncertainty, 1σ	Average Uncertainty, 1σ, %	Minimum Attenuation	Maximum Attenuation	Minimum Uncertainty, 1σ	Maximum Uncertainty, 1σ	Minimum Uncertainty, 1σ, %	Maximum Uncertainty, 1σ, %
P	0.9919	0.0008	0.0850%	0.9816	0.9975	0.0003	0.0019	0.0263%	0.1984%
S	0.9941	0.0006	0.0602%	0.9867	0.9982	0.0002	0.0014	0.0186%	0.1408%
Cl	0.9929	0.0004	0.0450%	0.9827	0.9978	0.0001	0.0010	0.0139%	0.1057%
Ar	0.9944	0.0003	0.0345%	0.9862	0.9982	0.0001	0.0008	0.0106%	0.0811%
K	0.9954	0.0003	0.0276%	0.9887	0.9985	0.0001	0.0006	0.0085%	0.0649%
Ca	0.9962	0.0002	0.0224%	0.9906	0.9987	0.0001	0.0005	0.0069%	0.0527%

1.5 Chester, LabNet (CLN)

CLN[8] does calculate mass (homogeneous layer) absorption (referred to by CLN as "self absorption") uncertainties for the thin film standards and mass absorption plus particle size correction uncertainties for field filter samples. Size corrections are considered secondary mass absorption corrections after deposit thickness corrections have been performed. Mass absorption uncertainty predominates. The formula used by CLN differs from that used by Dzubay, Eldred, and Kellogg. For CNL:

$$\delta_a = \left[\left(\left(\delta_c^{\,2} + \delta_i^{\,2} + \delta_s^{\,2} \right)^{1/2} / A \right)^2 + \left(0.1 \;\; N_c / A^2 \right)^2 \right]^{1/2} / A_p \qquad (13)$$

δ_a = absorption correction uncertainty (counts)

δ_c = counting uncertainty (counts)

δ_i = spectral overlap uncertainty (counts)

δ_s = calibration uncertainty (counts)

N_c = corrected net counts

A = homogeneous absorption correction factor, 0<A<1

A_p = size correction factor, $0<A_p<1$

This equation was developed by Eric Miller when he was with CLN. The basis (considered statistical) of the derivation of this formula is uncertain since no documentation has been located as of this time nor have we been able to contact Eric Miller. The uncertainty values calculated by CNL for thin film standards and NIST SRM 2783 are shown in Table 10.

Realizing that these values are relatively high, CLN has reexamined the formula and decided it is too conservative. The term "+ $0.1N_c$" is the component that results in the high values. CLN has proposed to deconvolute the results reported to RTI/EPA to date in order to back out the current values for particle size/layer absorption uncertainty and replace them with new values agreed upon by the various involved XRF laboratories. The approach to be taken is as follows:

For simplification, let total uncertainty be calculated as

$$\delta_{net} = (\delta_c^{\,2} + \delta_l^{\,2} + \delta_s^{\,2})^{1/2} \qquad (14)$$

which includes the uncertainties for peak fit or counting uncertainty (δ_c), spectral overlap uncertainty (δ_l), and calibration uncertainty (δ_s). Chester's uncertainty formula for attenuation has been expressed as:

$$\delta_a = [\delta_{net} / A)^2 + (0.1N / A^2)^2]^{1/2} / A_p \qquad (15)$$

Now values for *A* and A_p have been empirically determined from a series of standards and the NIST SRM 2783, respectively. It is understood that these values are based on comparison of measured and expected values. Values used by CLN are shown in Tables 11 and 12.

Table 10. Uncertainty values calculated by CNL for thin film standards and NIST SRM 2783

Element	Thin film standard[a]	SRM 2783[b]
Na	15.0%	MDL
Mg	13.8%	14.1%
Al	13.5%	11.6%
Si	13.1%	11.5%
P	11.7%	MDL
S	12.4%	11.8%
Cl	11.6%	12.1%
K	11.7%	11.4%
Ca	11.6%	11.3%
Sc through Pb	5%	----

[a]self-absorption only
[b]self-absorption and particle size

Table 11. Values for mass absorption attenuation factor, A, determined empirically for each of the three CLN XRF instruments

	Particle size attenuation factor, A_p								
Mass	**Na**	**Mg**	**Al**	**Si**	**P**	**S**	**Cl**	**K**	**Ca**
2.88	0.99	0.99	1.00	1.00	1.00	1.00	1.00	1.00	1.00
15.45	0.97	0.98	0.99	0.99	0.99	0.99	0.99	1.00	1.00
18.94	0.97	0.98	0.98	0.99	0.99	0.99	0.99	1.00	1.00
24.55	0.95	0.97	0.98	0.98	0.98	0.99	0.99	0.99	1.00
38.79	0.92	0.95	0.96	0.97	0.97	0.98	0.99	0.99	0.99
61.86	0.89	0.93	0.95	0.96	0.97	0.98	0.98	0.99	0.99

Table 12. Values for particle size attenuation factor, A_p, determined empirically for each of the three CLN XRF instruments.

Element	Chester XRF #770	Chester XRF #771	Chester XRF #772
Na	0.61	0.57	0.65
Mg	0.68	0.66	0.75
Al	0.79	0.79	0.82
Si	0.96	0.93	1.00
P	1.00	1.00	1.00
S	1.00	1.00	1.00
Cl	1.00	1.00	1.00
K	1.00	1.00	1.00
Ca	1.00	1.00	1.00

The regression of a plot of empirically-determined values of *A* vs deposit density (ρ, ug/cm^2) allows the calculation of *A* for a specific filter loading. The concentration and uncertainty for each element in each sample has been and is currently reported as $N_a \pm \delta_a$. The concentration before correction for layer absorption and particle size (N_c) is then back-calculated as:

$N_c = N_a \times A \times A_p$.

One now solves for a new value of estimated total uncertainty, [$(\delta_c^2 + \delta_l^2 + \delta_s^2)^{1/2}$], for the measured value uncorrected for layer absorption and particle size. That is,

$$\delta_{net} = (((A_p \delta_a)^2 - ((0.1 N_c) / A^2)^2))^{1/2}) A \qquad (16)$$

The deconvoluted value can now be expressed as $N_c \pm \delta_{net}$, which is equivalent to the empirically derived value prior to size and absorption corrections. Now one can combine the new values of δ_a calculated by methods agreed upon by the XRF laboratories involved with δ_{net} to calculate a new total uncertainty.

1.6 IMPROVE (Paul Wakabayashi, UC-Davis)

1.6.1 Attenuation

Attenuation of the light elements is included in the calculation of concentration in the IMPROVE program.[9] The IMPROVE SOP, “”X-ray Fluorescence Analysis,” last modified

02/04/97, describes corrections of the data for the “shadowing effect of particles on filters”. These corrections were derived in the in the 1970’s through experimentation with a variety of substrates and deposits to derive values for expected filter and loading types. In Table 13 of Reference 9, the correction values reported for select elements with Z > 14 are shown in Table 13. These values of about 2% are consistent with the values reported for UC-Davis in Table 1.

Table 13. IMPROVE attenuation values for select elements Z > 14.

Element	Correction (reported as attenuation, i.e., 1/correcton)
S	0.99
K	0.98
Ca	0.98

1.6.2 Attenuation Uncertainty

IMPROVE does not include a calculation of attenuation uncertainty in its overall calculation of uncertainty. Uncertainty calculations provided by IMPROVE's SOP 351, Section 4.5.2.8 [5] are as follows. Equation (351-31) within this SOP gives the precision of concentration:

$$[\sigma(c)]^2 = c^2 * (f_s^{\,2} + f_a^{\,2} + f_v^{\,2}) \qquad (17)$$

where,

σ(c) = precision of concentration

c = concentration

f_s = statistical fractional precision given by SOP Eqn. (350-30):

$$f_s^{\,2} = \frac{1}{N}\left(1 + 2\frac{N_b}{N}\right)$$

f_a = component of analytical precision that is a constant fraction (IMPROVE has used 0.04 for XRF since 1988)

f_v = fractional volume precision = fractional flow precision

The discussion on page A-48 of SOP 351 states: "The precision is calculated separately for each variable at the time of spectral analysis using f_a=0.04 and f_v=0.03. The quadratic sum of these two is 0.05. At small concentrations the statistical term is dominant, while at large concentrations the precision approaches 5%."

IMPROVE data (plots of reported uncertainty vs. concentration) have been examined and the uncertainties estimated from these plots for a range of real-world concentrations are shown in Table 14. This table show slopes of about 5% for the elements Al, Si, Cl, S, K and Ca, agreeing with the equation in the IMPROVE SOP (total concentration-proportional variation is a function of f_a and f_v).

Table 14. IMPROVE uncertainty values estimated from real-world data.

Element	Estimated uncertainty
Na	23% (very scattered data)
Mg	29% (very scattered data)
Al	5.8%
Si	5.3%
Cl	5.8%
S	4.9%
K	5.0%
Ca	5.0%

2.0 SUMMARY

A number of summary statements can be made regarding the method of calculation of attenuation by the different XRF laboratories:

- Dzubay and Nelson considered the fine particles and the coarse particles separately. They determined attenuation for fine particles with the homogeneous layer model and the attenuation for the coarse particles with the particle size model.

- Eldred considered only fine particles. He assumed the high end of the size distribution of the $PM_{2.5}$ contained coarse particles since there is overlap with the low end of the PM_{10} size distribution. He determined attenuation for the light elements using both the homogeneous layer model and the particle size model. Previously he applied both models; he has since expressed uncertainty about using both since he has data that indicate that most large particles will be free standing, that is, not included as part of a layer. He has left this issue unresolved.

- Kellogg also considered only fine particles. He assumed the high end of the size distribution of the $PM_{2.5}$ contained coarse particles since there is overlap with the low end of the PM_{10} size distribution. He determined attenuation for the light elements using both the homogeneous layer model and the particle size model; he applied the particle size model to elements with $Z = 11$ to 14 and the homogeneous layer model to elements with $Z > 14$.

- CLN determined attenuation due to mass (homogeneous layer) empirically from measurements with analytical standards and attenuation due to particle size empirically from measurements with a NIST Standard Reference Material. The total attenuation for each of the light elements was taken as the product of the two attenuation values.

- IMPROVE determined attenuation for the light elements empirically on the basis of tests with a number of laboratory-prepared filters in the 1970's.

The results of these different approaches are summarized in Tables 15 and 16. Dzubay and Nelson applied only the homogeneous layer model to the fine ($PM_{2.5}$) particles, and therefore only these data of Dzubay and Nelson can be compared to the data of Eldred and Kellogg. We do see that the attenuation values for the homogeneous model for Z > 14 agree well. If one looks back at Table 2, we see that they would not agree if we used the loading of 500 μg/cm^2. This is because such a large deposit (500 μg/cm^2) happens to attenuate x-rays comparably to 1-2 μm particles containing Al and Si. Eldred and Kellogg show similar values for attenuation for Al and Si calculated with the particle size model, even though the composition assumptions are different.

The uncertainties for these values were also calculated differently by each group. The variations in composition that served as a basis for these uncertainty calculations are summarized in Table 17. Unfortunately, Dzubay and Nelson did not publish (see Table 2) uncertainty values for their mass attenuation values determined with a filter at 100 μg/cm^2. Their uncertainty values for a filter at 500 μg/cm^2 for P through Ca ranged from about 5% to about 1%; these values cannot be compared to the homogeneous mass attenuation uncertainties of Kellogg because of the very different mass loading.

3.0 PROPOSAL

3.1 Particle Size Model

Along with John Rhodes[2], Tom Dzubay laid the fundamentals for calculating the effects of the physical structure and composition on attenuation of x-rays in x-ray spectrometry. Eldred and Kellogg advanced the work of these early researchers by considering the fact that the high end of the fine particle distribution will contain coarse particles since there is considerable overlap between the high end of the $PM_{2.5}$ distribution and the low end of the PM_{10} distribution. Kellogg has taken this concept a step farther by assuming that crustal particles containing the elements Na, Mg, Al, and Si predominate at the high end of the fine particle distribution. It is understood that the most common crustal minerals are the silicates - e.g., quartz SiO_2,

Table 15. Summary of values for attenuation and attenuation uncertainty from Dzubay and Nelson, Eldred, and Kellogg laboratories

Element	Dzubay and Nelson Models				Eldred Models				Kellogg Models			
	Homo. Layer[a]		Particle Size[b]		Homo. Layer		Particle Size		Homo. Layer		Particle Size	
	A	δ_a	A	δ_a	A	δ_a	A[c]	δ_a	A	δ_a	A	δ_a
Na	---	---	---	---	0.93	---	---	---	---	---	0.62	0.035 (5.6%)
Mg	0.90	---	---	---	---	---	---	---	---	---	0.65	0.044 (6.8%)
Al	0.93	---	0.41	0.12 (29%)	0.97	---	0.84-0.85	0.08 (1%)	---	---	0.76	0.032 (4.2%)
Si	0.95	---	0.48	0.15 (31%)	0.98	---	0.85-0.91	0.06 (7%)	---	---	0.80	0.032 (4.0%)
P	0.96	---	0.58	0.24 (41%)	0.99	---	---		0.99	0.003 (0.3%)	---	---
S	0.97	---	0.64	0.22 (34%)	0.99	---	0.99-0.99	0%	0.99	0.002 (0.2%)	---	---
Cl	0.96	---	0.70	0.20 (29%)	0.99	---	---		0.99	0.001 (0.1%)	---	---
K	0.98	---	0.78	0.15 (19%)	0.99	---	0.97-0.98	0.01 (1%)	0.99	0.001 (0.1%)	---	---
Ca	0.98	---	0.81	0.13 (16%)	0.99	---	0.99-0.96	0.03 (3%)	0.99	0.001 (0.1%)	---	---

[a] For fine ($PM_{2.5}$) particles only at 100 $\mu g/cm^2$ (see Table 2)
[b] For coarse (PM_{10}) particles only
[c] "All oxide" to "soil"

Table 16. Summary of values for attenuation and attenuation uncertainty from CLN and IMPROVE

Element	CLN Models								IMPROVE Model	
	Homo. Layer				Particle Size				Homo. Layer / Particle Size	
	A for areal mass, μg/cm^2			δ_a	A_p for XRF #			δ_a	A[a]	δ_a
	15.5	30.9	61.9		770	771	772			
Na	0.96	0.95	0.89	15%	0.61	0.57	0.65	MDL	0.93	None Reported
Mg	0.98	0.96	0.93	13.8%	0.68	0.66	0.75	14.1%	0.82	
Al	0.99	0.97	0.95	13.5%	0.79	0.79	0.82	11.6%	0.86	
Si	0.99	0.98	0.96	13.1%	0.96	0.93	1.0	11.5%	0.91	
P	0.99	0.98	0.97	11.7%	1.0	1.0	1.0	MDL	0.98	
S	0.99	0.98	0.98	12.4%	1.0	1.0	1.0	11.8%	0.99	
Cl	0.99	0.99	0.98	11.6%	1.0	1.0	1.0	12.1%	0.98	
K	1.0	0.99	0.99	11.7%	1.0	1.0	1.0	11.4%	0.98	
Ca	1.0	1.0	0.99	11.6%	1.0	1.0	1.0	11.3%	0.98	

[a]Attenuation determined empirically from laboratory test filters prepared in the 1970's . Attenuation apparently arises from a mix of layer and particle effects.

Table 17. Variation in composition used as basis for determining uncertainty of attenuation

XRF Laboratory	Homogeneous Layer Model	Particle Size Model
Dzubay and Nelson	Non-measured mass varied from $C_6H_{10}O_5$ to C_6H_6 to O (oxygen only)	Varied particle composition from botanical soil[b] to almandine (quartz to almandine for Al and Si)
Eldred	No uncertainty calculated. Assumed average $PM_{2.5}$ composition based on 15,000 samples[a]	No uncertainty calculated but did calculate attenuation for both all oxides and soil[c]
Kellogg	For Z > 14, non-measured mass varied from $C_6H_{10}O_5$ to C_6H_6 to O (oxygen only)	For Z = 11 to 14, calculated range of attenuations based on all reasonable minerals that would contain the element of interest
CLN	Based on statistical model	Based on statistical model

[a] 4.8% H, 25.3% C, 15.1% N, 38.0% O, 9.4% S, 1.45% Al, 3.19% Si, 0.78% K, 0.86% Ca, 0.85% Fe, 0.08% Ti, 0.06% Zn, < 0.05% V to Sr
[b] 95.7% $C_6H_{10}O_5$, 2% Ca, 1.5% K, 0.6% Mg, 0.2% P, and 0.03% Fe
[c] 50% O, 24% Si, 11% Al, 3%, 5% Ca, 6% Fe, 0.6% Ti, 0.1% Mn

aluminosilicates - e.g., K-feldspar (orthoclase) $KAlSi_3O_8$, and oxides - e.g., hematite Fe_2O_3; oxygen at 46 weight %, 63 atomic % and silicon at 28 weight %, 21 atom % predominate. Al, Fe, Ca, Na, K and Mg follow in descending concentration. If we accept Kellogg's premise, then it makes good sense to consider the composition of these large particles as a mix of all likely minerals as did Kellogg. Of the light elements, P and Cl are generally at very low levels in $PM_{2.5}$; the exception is high chloride in coastal samples. S as sulphate will most likely be found as a condensate particle and therefore not in the upper end of the fine particle distribution. It is therefore proposed that the Kellogg particle size model for Na, Mg, Al, and Si be accepted. The mixtures of minerals used to determine the ranges and thus uncertainties of the attenuations could be refined through consultation with mineralogists and XRF researchers, but the changes in the attenuation uncertainty values already presented by Kellogg are likely to be small. Also, by assuming mixtures that contain all reasonable minerals that include the element of interest, Kellogg has a model that should represent an approximate composite of relevant minerals from across the U.S.

- Alumino-silicates -- clays (e.g., kaolinite, montmorillinite, illite, and gibbsite; will vary among Ca-, Na-, and K-rich) from chemical weathering of feldspar; perhaps small amounts of residual (parent) feldspar, quartz, and muscovite mica as physical weathering products

- Iron oxides – (e.g., hematite and limonite) from chemical weathering of a wide range of ferro-magnesium minerals (amphiboles and pyroxenes); also, perhaps a small amount of residual (parent) ferro-magnesium parent minerals, particularly hornblende, augite, olivine, and biotite mica as physical weathering products

- Ca- and Mg-carbonates – calcite, gypsum

3.2 Homogeneous Layer Model

It is proposed that the attenuation of the elements with Z > 14 be determined using the homogeneous layer model. The decision to be made is that of the composition of the elements or material not measured by XRF. Earlier in this paper, it was reported that about 85% of the fine particulate was not measured by XRF. Eldred reports these materials from IMPROVE as:

4.8% H, 25.3% C, 15.1% N, and 38.0% O.

Table 18 shows results for the $PM_{2.5}$ species measured at RTI for $PM_{2.5}$ STN Batches 60 through 72.

Table 18. $PM_{2.5}$ species greater than 0.1% of GRAV measured by RTI in STN Batches 60 through 72.

		Not Blank Corrected					Blank Corrected	
Analysis	**Analyte**	**Average**	**St Dev**	**Count**	**RSD**	**% of Grav**	**Average**	**% of Grav**
Cations - $PM_{2.5}$ (NH4, Na, K)	Ammonium	17.0737	16.1453	16216	95%	9.62%	17.0562	9.99%
Cations - $PM_{2.5}$ (NH4, Na, K)	Potassium	0.5777	1.4138	16216	245%	0.33%	0.5707	0.33%
Cations - $PM_{2.5}$ (NH4, Na, K)	Sodium	1.3227	3.7836	16209	286%	0.74%	1.0683	0.63%
Mass - $PM_{2.5}$	Particulate matter 2.5u	177.5626	138.0879	16107	78%	100.00%	170.7594	100.00%
Nitrate – $PM_{2.5}$	Nitrate	18.0625	26.7017	15489	148%	10.17%	17.7250	10.38%
OC/EC	Elemental carbon	7.2247	6.6922	16231	93%	4.07%	7.0536	4.13%
OC/EC	Organic carbon	43.1401	23.6521	16231	55%	24.30%	32.6754	19.14%
Sulfate – $PM_{2.5}$	Sulfate	40.0295	39.1034	16216	98%	22.54%	39.6870	23.24%
Trace elements	Aluminum	0.2498	0.7363	16178	295%	0.14%	0.2365	0.14%
Trace elements	Calcium	0.7402	1.3021	16178	176%	0.42%	0.7305	0.43%
Trace elements	Chlorine	0.3559	1.4746	16178	414%	0.20%	0.3508	0.21%
Trace elements	Iron	1.2060	1.7362	16178	144%	0.68%	1.1830	0.69%
Trace elements	Potassium	0.9563	1.6935	16178	177%	0.54%	0.9503	0.56%
Trace elements	Silicon	1.0509	2.0912	16178	199%	0.59%	1.0247	0.60%
Trace elements	Sodium	0.7269	1.3911	16174	191%	0.41%	0.6693	0.39%
Trace elements	Sulfur	16.1082	17.7246	16178	110%	9.07%	16.0934	9.42%
Trace elements	Zinc	0.2037	0.4072	16178	200%	0.11%	0.2014	0.12%

Here the totals are estimated as:

3% H based on ammonium and OC as $C_6H_{10}O_5$, 23% C, 10% N, and about 36% O based on SO_4^{-2}, NO_3^{-1}, and OC as $C_6H_{10}O_5$.

These results agree reasonably well with those of Eldred using IMPROVE data. Dzubay and Kellogg determined their uncertainties assuming variation in the non-XRF measured materials going from $C_6H_{10}O_5$ to C_6H_6 to O (oxygen only). It would seem reasonable to take advantage of the extra analysis information (from OC/EC and ion analyses) and extend this model to include the

variation of H, C, and O to determine the attenuation uncertainties. Nitrogen could be included, but it will make no perceptible difference because of the low absorption characteristics of this species.

3.3 Proposed Effort for Harmonization

3.3.1 Particle Size Model for Na, Mg, Al and Si.

The attenuation values determined with the particle size model for the various XRF's used are dependent upon:

- The mass absorption coefficients for each element (which depend upon the excitation energy, i.e., the type of primary anode or secondary target used to generate the excitation x-rays)
- The weight fraction of each element present assuming a "known" set of mineral particles
- The composition of the particles and their densities based on the mineral type
- The range of particle sizes based on the nominal $PM_{2.5}$ particle size distribution

The attenuation values are instrument dependent (excitation energies, source and detector geometry) and must be calculated separately by each laboratory; the range of excitation conditions is shown in Table 19. As to the uncertainty, it is proposed that the best choice, given the high values for peak/curve fitting uncertainty, would be to accept the values of Kellogg as calculated with his chosen set of minerals. As an improvement of this proposal, Kellogg agreed to calculate the range of attenuation values for the elements Na, Mg, Al, and Si that would be measured on the XRF's used at RTI and CLN for a set of pre-chosen mineral particles. These values are presented in Table 20. With the mineral set being comprehensive, it is reasonable to assume the range of values is between 2 and 3 σ as done by Kellogg. As noted, the changes in attenuation uncertainty with changes in the instrument operating parameters are minimal. Also, the small differences in attenuation uncertainties will not be significant when these uncertainties are combined with the fitting uncertainty, the calibration uncertainty, and the field sampling uncertainty, as described below.

Table 19. Excitation conditions used for $PM_{2.5}$ analyses by different laboratories

Condition	Anode	Secondary Target or Filter	Elements
RTI ThermoNoran QuanX EC XRF #1, #2, and #3			
1	Rh anode,	No filter	Na, Mg, Al, Si
2	Rh anode,	Graphite filter	P, S, Cl, K, Ca, Sc
3	Rh anode,	Pd thin filter	Ti, V, Cr, Mn, Fe, Co, Ni, Cu, Zn, Cs, Ba, La, Ce, Sm, Eu, Tb, Hf
4	Rh anode,	Pd thick filter	Ga, As, Se, Br, Rb, Sr, Y, Zr, Nb, Mo, Ta, W, Ir, Au, Hg, Pb
5	Rh anode,	Cu thick filter	Ag, Cd, In, Sn, Sb
Chester Labnet Kevex 770 and 772			
0	Rh anode,	Cellulose prefilter	Na, Mg, Al, Si, P
1	Rh anode,	Ti secondary target	S, Cl, K
2	Rh anode,	Fe secondary target	Ca, Sc, Ti, V, Cr
3	Rh anode,	Ge secondary target	Mn, Fe, Co, Ni, Cu, Zn, Sm, Eu, Tb
4	Rh anode,	Rh prefilter	Ga, Ge, As, Se, Br, Rb, Sr, Y, Zr, Nb, Mo, Hf, Ta, W, Ir, Au, Hg, Pb
5	Rh anode,	W prefilter	Rh, Pd, Ag, Cd, In, Sn, Sb, Te, I, Cs, Ba, La, Ce
Chester Labnet Kevex 771			
1	Rh anode,	Cellulose prefilter	Na, Mg, Al, Si, P
2	Rh anode,	Fe secondary target	Sr, Cl, K, Ca, Sc, Ti, V, Cu
3	Rh anode,	Ge secondary target	Mn, Fe, Co, Ni, Cu, Zn, Sm, Eu, Tb
4	Rh anode,	Rh prefilter	Ga, Ge, As, Se, Br, Rb, Sr, Y, Zr, Nb, Mo, Hf, Ta, W, Ir, Au, Hg, Pb
5	Rh anode,	W prefilter	Rh, Pd, Ag, Cd, In, Sn, Sb, Te, I, Cs, Ba, La, Ce
EPA/Alion LBL XRF			
1	W tube	Ti fluorescer	Al, Si, P, S, Cl, Ar, K, Ca
2	W tube	Co fluorescer	S, Cl, Ar, K, Ca, Sc, Ti, V, Cr, Mn, Ce, La
3	W tube	Mo fluorescer	Mn, Fe, Co, Ni, Cu, Zn, Ga, Ge, As, Se, Br, Rb, Sr, W, Pt, Au, Hg, Tl, Pb
4	W tube	Sm fluorescer	Rb, Sr, Y, Zr, Nb, Mo, Rh, Pd, Ag, Cd, In, Sn, Sb, Te, I, Cs, Ba
IMPROVE Laboratory XRF			
1	Cu anode	None	Na, Mg, Al, Si, P, Cl, K, Ca, Ti, V, Cr, Mn, Fe
2	Mo anode	None	Ni, Cu, Zn, Ga, As, Se, Br, Rb, Sr, Zr, Nb, Hg, Pb

Table 20. $PM_{2.5}$ attenuation uncertainties for Ma, Mg, Al, and Si with RTI and CLN XRF spectrometers

Element	RTI Thermo QuanX		CLN Kevex	
	1σ	2.5σ	1σ	2.5σ
Na	0.0454 (6.5%)	0.1134 (16.3%)	0.0469 (6.9%)	0.1174 (17.2%)
Mg	0.0341 (4.6%)	0.0852 (11.5%)	0.0354 (4.8%)	0.0884 (12.1%)
Al	0.0334 (4.5%)	0.0836 (11.2%)	0.0346 (5.2%)	0.0866 (13.0%)
Si	0.0338 (4.3%)	0.0845 (10.7%)	0.0331 (4.7%)	0.0828 (11.9%)

3.3.2 Homogeneous Layer Model for Z > 14

The attenuation values determined with the homogeneous layer model for the various XRF's used are dependent upon:

- The mass absorption coefficients for each element (which depend upon the excitation energy, i.e., the type of primary anode or secondary target used to generate the excitation x-rays)
- The areal density of the deposit (gm/cm^2)
- The weight fraction of each element present assuming a "known" set of mineral particles

As with Na, Mg, Al, and Si, the attenuation values determined for Z > 14 are instrument dependent (excitation energies, source and detector geometry). They are also sample dependent, and must be calculated separately for each sample. Here too, it is proposed that we use the values of Kellogg for uncertainties for Z > 14. To assure greater accuracy, the homogeneous layer uncertainty could be recalculated for each sample assuming a mutually acceptable variation in non-XRF species or material. As noted above, this variation would reflect the range of values for H, C, and O found in $PM_{2.5}$. With the non-XRF species actually being measured, it is reasonable to assume the range of uncertainty values is between 2 and 3 σ. These calculations could potentially be done using the software developed by Dzubay and advanced by Kellogg using only the instrument parameters as the starting point. The uncertainties, if significantly different between laboratory instruments, would be applied to the analysis data from whence they came. If they are not significantly different between laboratories, an average value would be applied to all the $PM_{2.5}$ data for these elements with Z > 14. But, in fact, based on the data presented in Table 16, little difference in attenuation for elements Z > 14 is expected between laboratories. Also, attenuations for Z > 14 for typical

ambient aerosol samples are very close to unity, and so the uncertainties are almost negligible. Thus the values presented by Kellogg are to be used in the harmonization.

3.3.3 Total Uncertainty

The attenuation uncertainties provided by Kellogg will be combined with the uncertainties of curve fitting, calibration (5%), and field sampling (5%) to arrive at uncertainties for each sample. These final calculations will be done on the RTI data as now available and on the CLN data after backing out the current values for attenuation uncertainty as described above.

Figures 2 through 5 illustrate the effects of recalculating the total uncertainties for data from RTI [XRF 1 and XRF 2] and Chester LabNet [770 and 771]; IMPROVE [IMP] XRF uncertainty data that are not harmonized are shown for comparison purposes. The IMPROVE concentration and uncertainty values shown are taken from the VIEWS website; data was taken from randomly chosen sites in order to illustrate the dependency between concentration and reported uncertainty. Figures 2 and 4 show the uncertainties as originally reported by the respective laboratories. Figures 3 and 5 show total uncertainty for RTI and Chester Labnet data with the proposed changes and additions; again, the IMPROVE data are shown without harmonization. It should be noted that the total uncertainty of the IMPROVE XRF data is based on the uncertainty of the determination of the analyte x-ray emission peak areas and 4% for calibration uncertainty and does not include attenuation uncertainty. Harmonization of the IMPROVE data principally through inclusion of attenuation uncertainties (see Section 1.2.3) would bring the IMPROVE total uncertainty values close to those of the harmonized RTI and Chester LabNet values, as shown in Figures 6 and 7. It is our understanding that Warren White of UC-Davis is reevaluating the IMPROVE method for determining uncertainties and may propose changes in the future.

The figures show a considerable improvement in the comparability of the total uncertainties as a result of this approach to harmonization. As noted, the values for δ_a vary between researchers, and these values could potentially be refined using improved estimates of the composition and structure of the $PM_{2.5}$ samples. However, the effects of these revisions on overall uncertainty will be small.

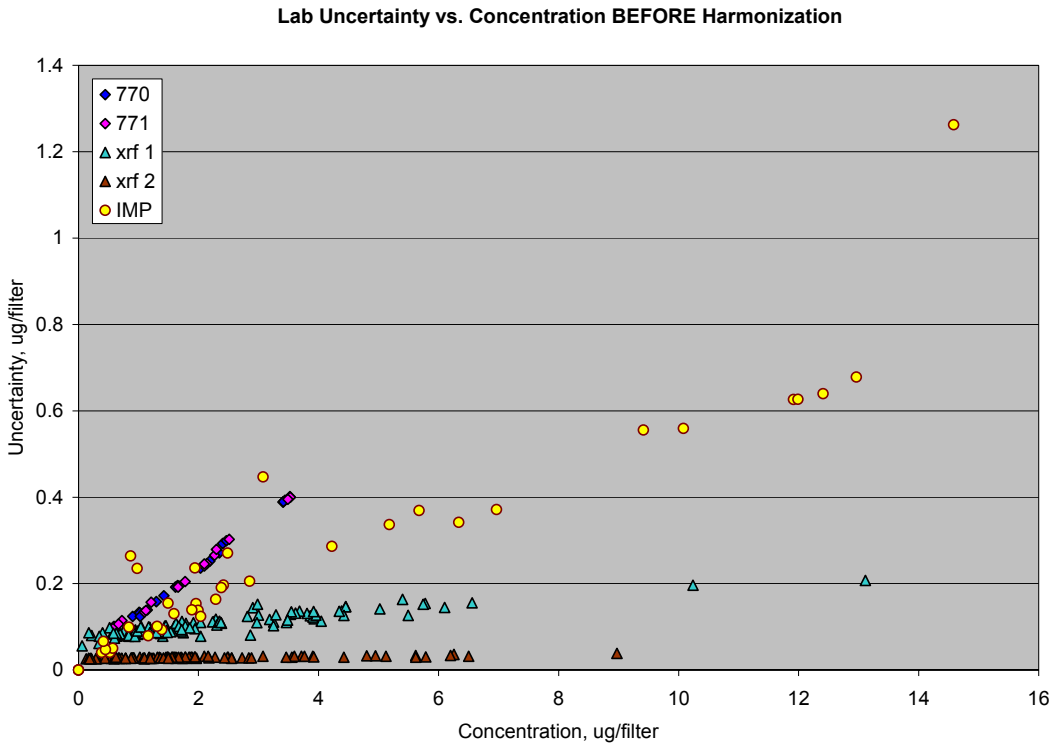

Figure 2. Silicon Laboratory Uncertainty before Harmonization.

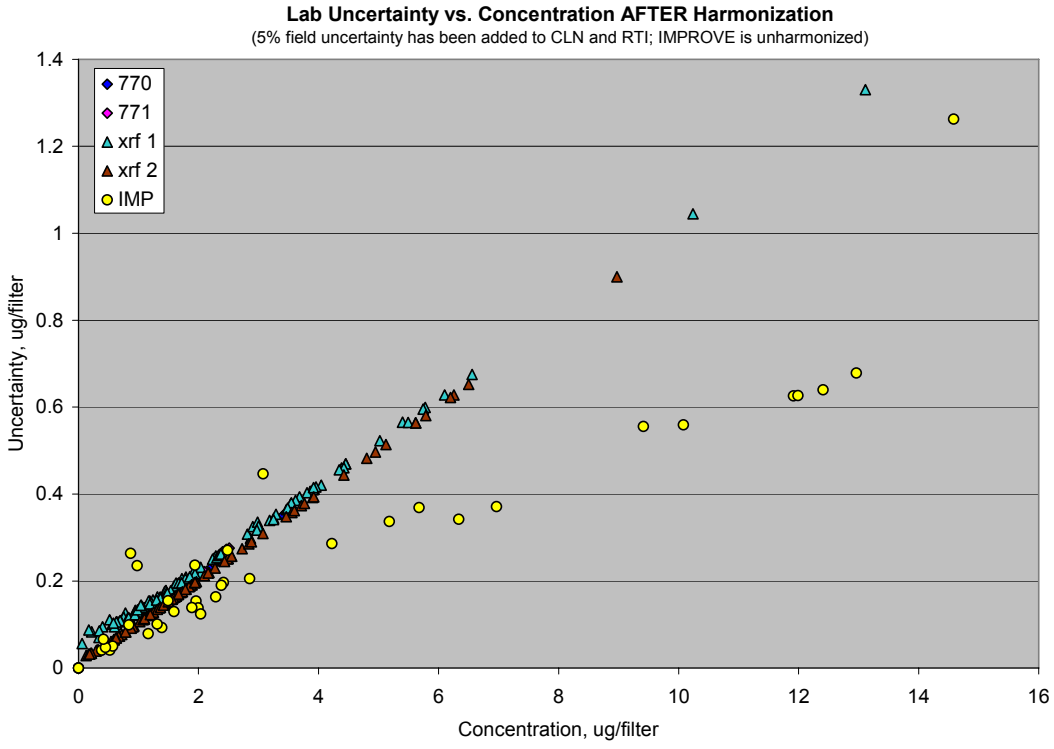

Figure 3. Silicon Total Uncertainty after Harmonization (IMPROVE data not harmonized).

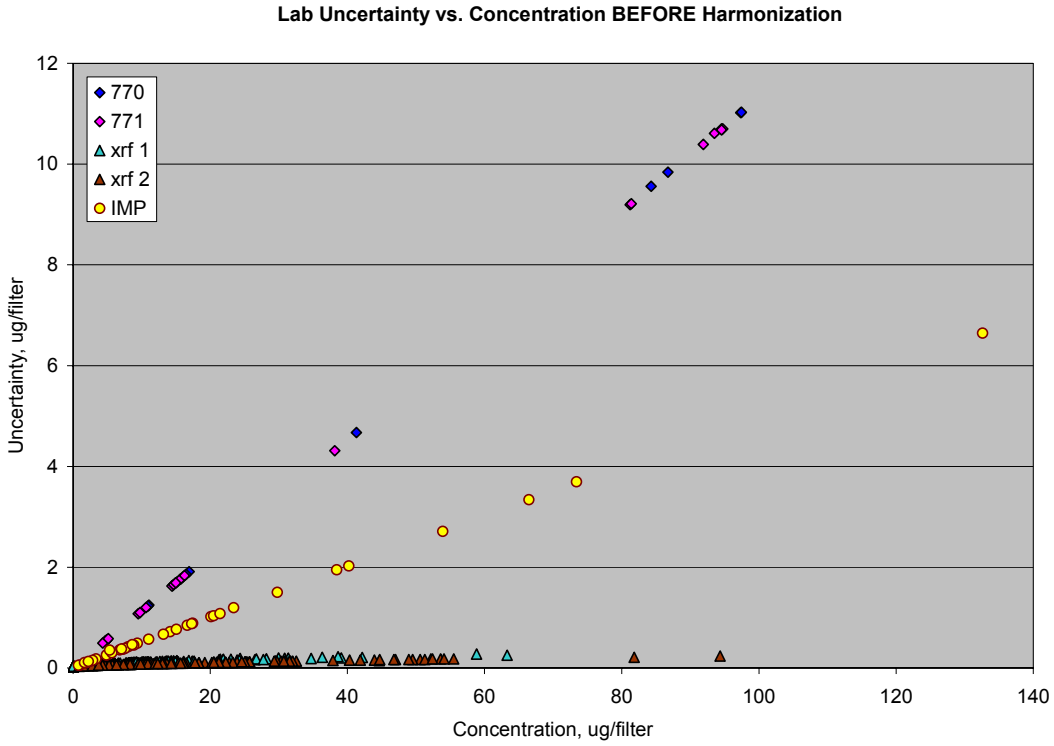

Figure 4. Sulfur Laboratory Uncertainty before Harmonization.

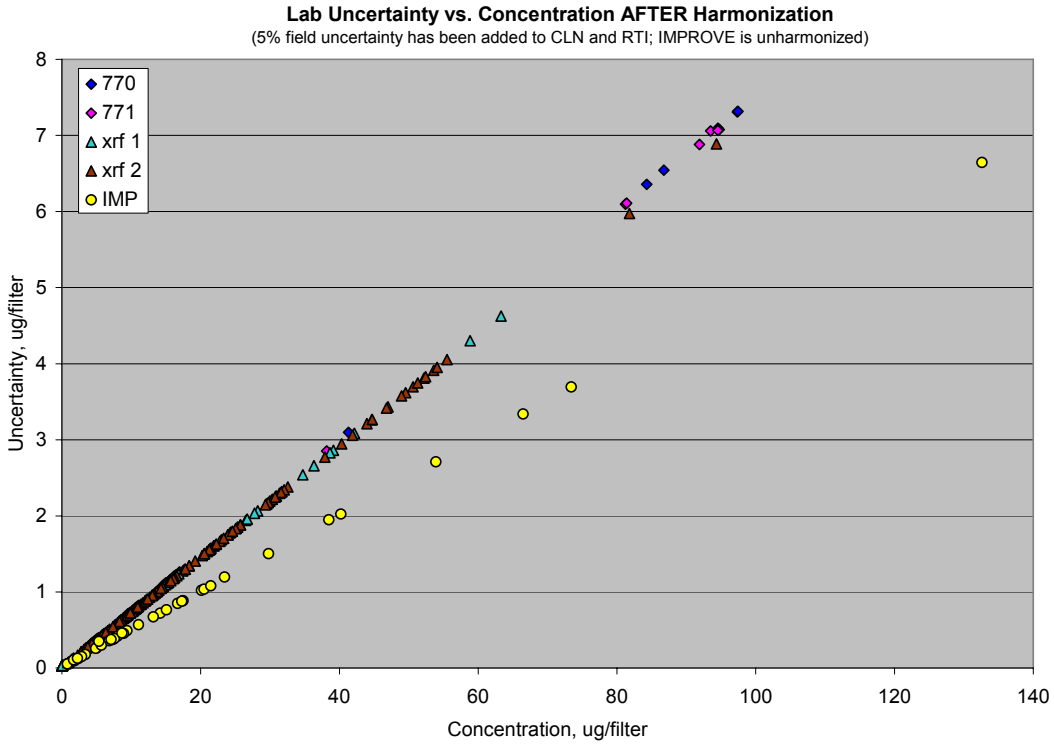

Figure 5. Sulfur Total Uncertainty after Harmonization (IMPROVE data not harmonized).

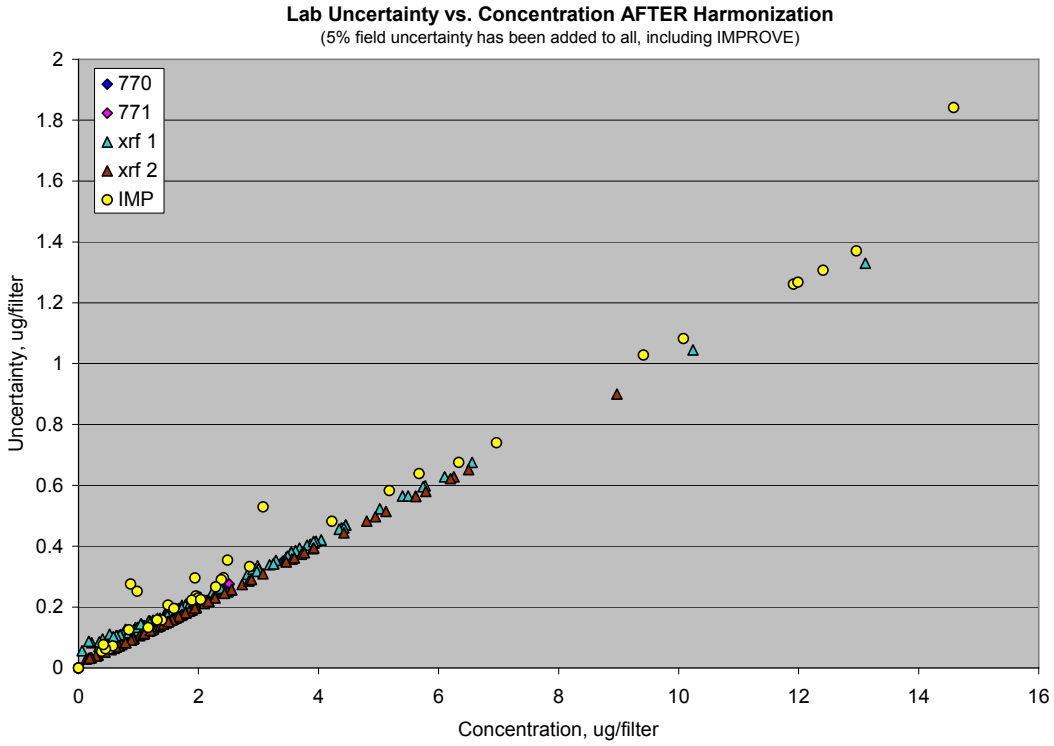

Figure 6. Silicon Total Uncertainty after Harmonization (IMPROVE data harmonized).

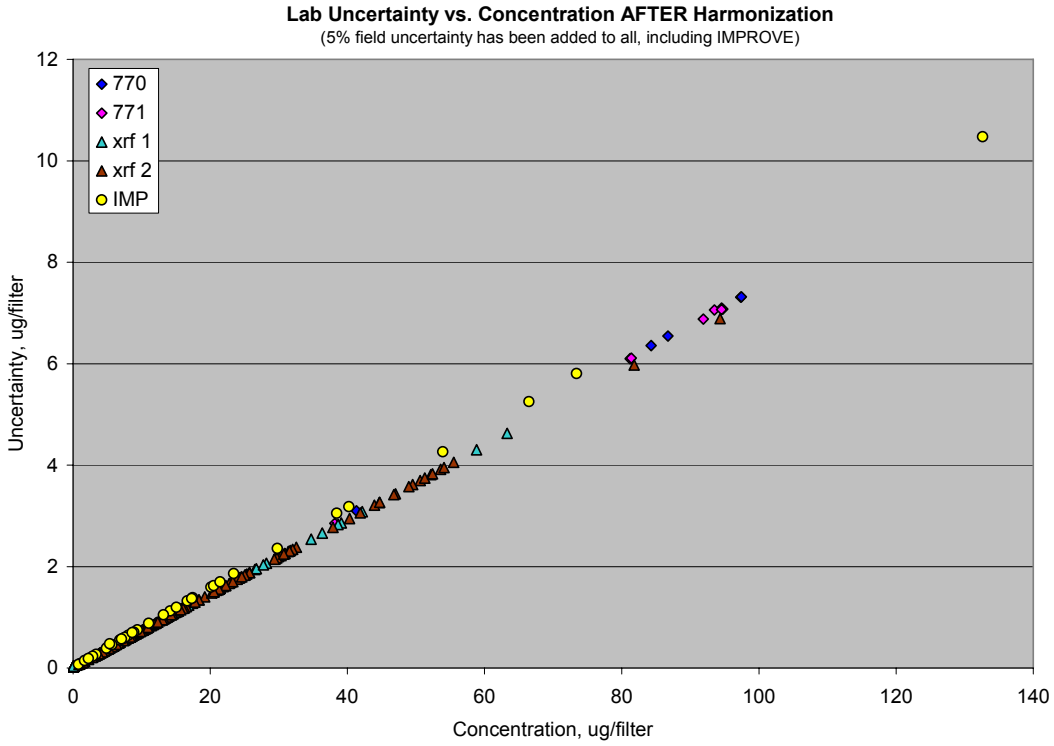

Figure 7. Sulfur Total Uncertainty after Harmonization (IMPROVE data harmonized).

4.0 REFERENCES

(1) Dzubay, T. G. and R. O. Nelson, "Self Absorption Corrections for X-ray Fluorescence Analysis of Aerosols." Advances in X-Ray Analysis, ed. W. L. Pickles, et al., Plenum Publishing Corp., New York, N.Y., 18:619, 1975.

(2) Rhodes, J.R. and C.B. Hunter, "Particle Size Effects in X-ray Emission Analyses: Simplified Formulas for Certain Practical Cases", X-ray Spectrometry 1:113-117 (1972).

(3) L.B. Lockhart, Jr., and R.L. Patterson, Jr., and W.L. Anderson, "Characteristics of Air Filter Media Used for Monitoring Airborne Radioactivity", NRL Report 6054 (1963).

(4) Eldred, Bob, "X-ray Matrix Corrections", CNL-IMPROVE Memo, University of California – Davis, May, 2004.

(5) Kellogg, R. B., "X-ray Fluorescence Analysis of Fine Ambient Aerosols at the USEPA, RTP, NC." Alion Science and Technology, April 2005.

(6) Kellogg, R. B., "Error Analysis in EDXRF of Ambient Aerosols." Alion Science and Technology.

(7) Cooper, John, personal communication. Cooper Environmental Services, August, 2005.

(8) Sarver, R., personal communications. Chester LabNet, May, July, September, December, 2005,

(9) IMPROVE SOP 301, "X-ray fluorescence Analysis." Dates modified: 10/24/96 by EAR and 02/04/97 by RAE.

(10) IMPROVE SOP 351, "Data Processing and Validation." Dates modified: 12/09/96 by EAR and 10/09/97 by RAE.

Attachment 1

Example of mass absorption attenuation correction.

Micromatter 4944 is a thin-film vapor-deposited Sulfur standard with chemical composition CuS_x where:

Cu = 43.9 $\mu g/cm^2$ and
S = 13.0 $\mu g/cm^2$ and
CuS_x = 43.9 + 13.0 = 56.9 $\mu g/cm^2$

The weight percent for each is then calculated:

$$Cu = \frac{43.9}{56.9} = .772$$

$$S = \frac{13.0}{56.9} = .228$$

The excitation (μ) radiation is Rh Lα (2.7 KeV) and the fluorescent radiation (μ') is S Kα (2.31 KeV)

The excitation occurs at an angle 21° from parallel to the sample: θ = 21° ; cscθ = 1.071

The fluorescent radiation enters the detector colimator at an angle 45° from parallel to the sample: θ = 45° ; cscθ = 1.414

From the table of mass absorption coefficients we find:

μS = 1770 cm^2/g which represents the thickness of sulfur at which ½ of the excitation energy (Rh Lα) would be absorbed by sulfur.

μCu = 885 cm^2/g

μ'S = 250 cm^2/g which represents the thickness of sulfur at which ½ of the fluorescent energy (S Kα) would be absorbed by sulfur

μ'Cu = 1350 cm^2/g

μ = (1770)(.228) + (885)(.772) = 1086.8

μ' = (250)(.228) + (1350)(.772) = 1099.2

$\underline{\mu}$ = μ cscθ + μ' cscθ' = (1086.8)(1.071) + (1099.2)(1.414) = 2718.2

m = deposit areal density in g/cm^2 = 56.9 x 10^{-6}

$A = 1-e^{-\underline{\mu}m} / \underline{\mu}m$

$A = 1-e^{-(2718.2)(56.9x10-6)} / (2718.2)(56.9 \times 10^{-6}) = .9265$

The surface equivalent value (SEV) for sulfur used to determine the calibration factor would then be:

13.0 x .9265 = 12.04 $\mu g/cm^2$

KeVex Absorption Table												
	Incom	Incom	Exit	Exit	Exit	Exit	Exit	Exit	Exit	Exit	Exit	Exit
	Rh La	Ti Ka	Na Ka	Mg Ka	Al Ka	Si Ka	P Ka	S Ka	Cl Ka	K Ka	Ca Ka	Ti Ka
csc	1.071	1.4142	1.4142	1.4142	1.4142	1.4142	1.4142	1.4142	1.4142	1.4142	1.4142	1.4142
C	116	26	1780	1050	640	400	263	175	125	61	45	26
O	275	63	4000	2440	1520	965	633	435	300	162	115	63
Na	650	163	8160	4925	3395	2100	1480	1030	715	366	276	163
Mg	850	212	580	350	4050	2660	1794	1330	930	490	367	212
Al	1035	263	850	500	330	3170	2223	1610	1130	595	450	263
Si	1265	328	1230	740	480	315	2645	1960	1375	735	556	328
P	1435	389	1640	1015	650	435	300	2180	1570	850	648	389
S	**1770**	453	2100	1320	795	525	355	**250**	1920	1030	671	453
Cl	190	512	2500	1570	960	635	435	300	210	1140	870	512
K	280	689	3425	2120	1300	855	593	425	305	162	606	689
Ca	320	780	3850	2380	1500	980	710	480	345	185	142	780
Ti	425	114	4680	2975	2000	1300	905	645	455	250	190	114
V	480	129	5050	3260	2200	1460	1020	730	520	280	215	129
Cr	550	153	5480	3510	2470	1670	1165	835	590	320	247	153
Mn	675	171	5895	3790	2700	1920	1310	935	665	360	279	171
Fe	700	193	6275	4100	2910	2040	1465	1070	760	410	317	193
Co	735	198	6640	4380	3070	2195	1565	1160	790	435	341	198
Ni	830	244	6800	4540	3140	2225	1675	1260	900	490	379	244
Cu	**885**	262	7550	5035	3450	2415	1780	**1350**	960	530	419	262
Zn	1050	292	0	5235	3645	2510	1915	1460	1130	595	480	292
Ga	1145	300	0	0	3810	2645	2025	1575	1225	700	508	300
Ge	1210	325	0	0	3995	2750	2145	1670	320	760	543	325
As	1310	340	1580	1020	0	2880	2490	1795	1420	820	595	340
Se	1380	380	1740	1110	0	3010	2620	1930	1530	925	660	380
Br	1410	480	1875	1190	840	0	2528	2060	1615	1025	703	480
Rb	1630	455	2200	1380	950	710	0	2330	1810	1190	805	455
Sr	1740	180	2400	1500	1020	760	0	2465	1910	1260	875	180
Y	1875	515	2555	1820	1080	810	648	0	2020	1310	938	515
Zr	1940	580	2755	1740	1155	855	688	0	2125	1390	995	580
Mo	0	720	3180	2005	1315	990	788	630	0	1540	1190	720
Pd	550	890	4100	2590	1675	1260	1000	800	590	0	683	890
Ag	585	925	4230	2700	1800	1350	1058	860	625	355	1365	925
Cd	620	1025	4660	2930	1880	1415	1120	890	665	385	0	1025
In	650	1065	4880	3080	1975	1480	1175	930	700	400	170	1065
Sn	720	1020	5300	3360	2280	1475	1235	990	760	435	348	1020
Sb	730	0	5510	3500	2355	1660	1310	1050	780	455	368	0
Te	770	0	5825	3650	2500	1740	1375	1100	825	480	385	0
I	805	265	0	3870	2645	1840	1453	1160	870	505	405	265
Cs	0	0	0	0	0	2010	0	0	0	0	0	0
Ba	940	310	0	0	0	2130	1680	1345	1010	585	473	310
La	980	325	0	0	0	2210	1760	1400	1055	610	495	325
Hg	0	880	0	0	0	0	0	0	0	0	1435	880
Pb	0	935	0	0	0	0	0	0	0	0	1500	935

This calibration factor will yield a SEV for sulfur for each sample, and must be then corrected for absorption based on the presence of each absorbing species. If these steps are not taken, and the 13.0 $\mu g/cm^2$ value is used for calibration, then the sulfur calibration factor will only be valid for samples with the same chemical composition and concentration of the standard. Chester applies this formula to all XRF standards containing Na, Mg, Al, Si, P, S, Cl, K, and Ca.